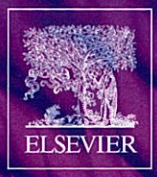

MICROBIOROBOTICS

Biologically Inspired Microscale Robotic Systems

Second Edition

Edited by
MinJun Kim
Anak Agung Julius
U Kei Cheang

Micro & Nano Technologies Series

Microbiorobotics

Microbiorobotics

Biologically Inspired Microscale Robotic Systems

Second Edition

Edited by

MinJun Kim

Anak Agung Julius

U Kei Cheang

ELSEVIER elsevier.com

Contents

Contributors

Walid Amokrane
HEI Centre campus, Châteauroux, France

Aaron T. Becker
University of Houston, Houston, TX, United States

Karim Belharet
HEI Centre campus, Châteauroux, France

David Cappelleri
Purdue University, West Lafayette, IN, United States

U Kei Cheang
Drexel University, Philadelphia, PA, United States

Jongeun Choi
Yonsei University, Seoul, South Korea

Sagar Chowdhury
Purdue University, West Lafayette, IN, United States

Antoine Ferreira
University of Orléans, Bourges, France

Peer Fischer
Max Planck Institute for Intelligent Systems, Stuttgart, Germany;
University of Stuttgart, Stuttgart, Germany

Jiwon Han
Chonnam National University, Gwangju, South Korea

Wuming Jing
Purdue University, West Lafayette, IN, United States

Anak Agung Julius
Rensselaer Polytechnic Institute, Troy, NY, United States

Sunghwan Jung
Virginia Tech, Blacksburg, VA, United States

Islam S.M. Khalil
The German University in Cairo, New Cairo City, Egypt

Dal Hyung Kim
Rowland Institute at Harvard University, Cambridge, MA, United States

Hoyeon Kim
Southern Methodist University, Dallas, TX, United States

MinJun Kim
Southern Methodist University, Dallas, TX, United States

Paul Seung Soo Kim
Drexel University, Philadelphia, PA, United States

Vijay Kumar
University of Pennsylvania, Philadelphia, PA, United States

Dejan Milutinović
University of California, Santa Cruz, Santa Cruz, CA, United States

Sarthak Misra
University of Twente, Enschede, The Netherlands

Yan Ou
Rensselaer Polytechnic Institute, Troy, NY, United States

Stefano Palagi
Max Planck Institute for Intelligent Systems, Stuttgart, Germany

Jong-Oh Park
Chonnam National University, Gwangju, South Korea

Sukho Park
Daegu Gyeongbuk Institute of Science and Technology, Daegu, South Korea

Tian Qiu
Max Planck Institute for Intelligent Systems, Stuttgart, Germany;
Swiss Federal Institute of Technology in Lausanne, Lausanne, Switzerland

Mahmut Selman Sakar
Swiss Federal Institute of Technology in Lausanne, Lausanne, Switzerland

Edward B. Steager
University of Pennsylvania, Philadelphia, PA, United States

Debora Walker
Max Planck Institute for Intelligent Systems, Stuttgart, Germany

Denise Wong
University of Pennsylvania, Philadelphia, PA, United States

Part 3

Biological Microrobots

Chapter 3

Development of active controllable tumor targeting bacteriobot

Jiwon Han*, Jong-Oh Park*, Sukho Park†
*Chonnam National University, Gwangju, South Korea
†Daegu Gyeongbuk Institute of Science and Technology, Daegu, South Korea

CHAPTER OUTLINE

3.1 FABRICATION AND SURFACE MODIFICATION OF BIOCOMPATIBLE MICROBEADS

A bacteriobot can provide a new theragnostic choice for cancer treatment with the active targeting properties of bacteria and contained therapeutic agents. Generally, a bacteriobot consists of the therapeutic part and the actuating part. The therapeutic part is the microstructure, composed of diagnostic or chemotherapeutic agents and biocompatible, biodegradable polymers. The microstructures using biocompatible materials, such as poly lactic-co-glycolic acid (PLGA), poly ethylene glycol (PEG), and liposome, served as micro cargos of agents for the imaging or therapy of tumors. In addition, the surface structural modification of the microstructures was performed by

coating with poly-L-lysine (PLL), O_2 plasma, bovine serum albumin (BSA), and biotin. Through the surface modification of microstructures, bacteriobots might show advanced motility through adjusted bacterial adhesion.

3.1.1 PEG microbeads and surface modifications

PEG is most extensively studied and it uses synthetic materials for drug delivery applications. It has many excellent properties for biomedical applications, such as biodegradability, biocompatibility, and flexibility. In addition, PEG has a stealth property to avoid its uptake by the reticuloendothelial system (RES) and to remain in the blood stream.

PEG microbeads containing anticancer agents or not were fabricated using various types of PEG, such as PEG-diacrylate (PEG-DA), PEG-Thiol (PEG-SH), and PEG-maleimide (PEG-Mal), with related chemicals for the assembly of PEG. PEG microbeads can be synthesized using various chemical and physical cross-linking and gelatin techniques, such as ionic interactions and photo-polymerization. However, although the photo-polymerization method is a widely used technique for hydrogels, it is unsuitable for a biological application. Because this method requires highly toxic photo-initiators and ultraviolet (UV) rays, they can cause undesirable reactions on cells. These undesirable effects can be reduced using physical cross-linking techniques or chemical cross-linking with non-toxic chemicals and a safe light source. Among various chemical cross-linking methods, the thiol-Michael reaction between nucleophiles and activated olefins is the most suitable, as it has the following advantages: it does not contain heat or light in the procedure, it does not generate byproducts, it shows rapid reaction rates, and it only requires a little amount of a catalyst [1]. In addition, microbead synthesis via the thiol-Michael reaction requires a relatively mild condition, a rapid cure, and a high conversion under a physiological environment. Consequently, the thiol-Michael technique becomes a significant chemical cross-linking method for the biological application of microbeads.

Using the thiol-Michael technique, two types of PEG—4 arm PEG-SH and 4-arm PEG-Mal—were fabricated, and Taxol-loaded PLGA nanoparticles were engaged in PEG microbeads for therapeutic microrobot fabrication [2]. Taxol-loaded PLGA nanoparticles were prepared through the solvent evaporation method and the lyophilization method. The mixture solution of PEG-SH and Taxol-loaded PLGA nanoparticles was produced. In addition, the micro-droplets of the mixture were fabricated by a micro-fluidic device and cross-linked with PEG-Mal. Consequently, 10-μm diameter drug-loaded PEG microbeads were produced (Fig. 3.1). Through the surface coating with PLL on the PEG microbeads, bacteria could be attached on the drug-loaded PEG microbeads.

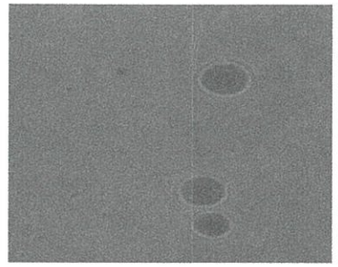

■ **FIGURE 3.1** Microscopy image of PEG microbeads [2].

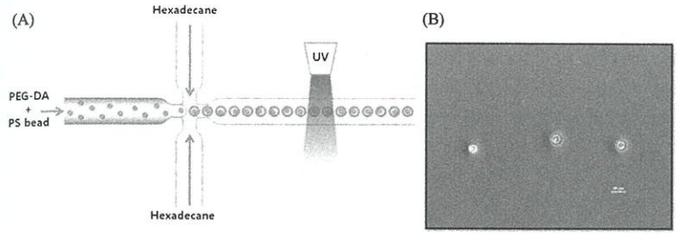

■ **FIGURE 3.2** Development of PEG-DA microbeads in a microfluidic channel system [4].

PEG is a hydrophilic polymer that can be polymerized by a photo-initiator, such as visible or UV light [3]. PEG microbeads (8.18 ± 3.4 μm diameter) using a PEG derivative, PEG-DA, and UV irradiation, were developed in a microfluidic channel system (Fig. 3.2) [4]. Recently, in the fabrication of microbeads using biocompatible polymers (e.g., PLGA, PEG), microfluidic channel systems have been widely used [5]. Those systems have many advantages for the fabrication of microbeads, such as a small sample requirement, relatively short reaction times, and high reproducibility [6]. In addition, the size and shape of the microbeads can be controlled through the regulation of the dimensions and flow rates of microfluidic channels [7]. The microfluidic channel using polydimethylsiloxane (PDMS) was prepared by conventional photo- and soft-lithography procedures [8]. For the fabrication of the microfluidic channel, first, an SU-8 cross-junction mold was produced through conventional photolithography procedures, such as SU-8 photo-resistor coating and UV irradiation through a pattern mask, developing step, and hard baking. Second, the PDMS cross-junction microfluidic channel pattern was obtained through soft-lithography procedures. Finally, the PDMS cross-junction microfluidic channel for the synthesis of PEG microbeads was completed through the attachment of the PDMS pattern to a glass substrate (Fig. 3.3) [4].

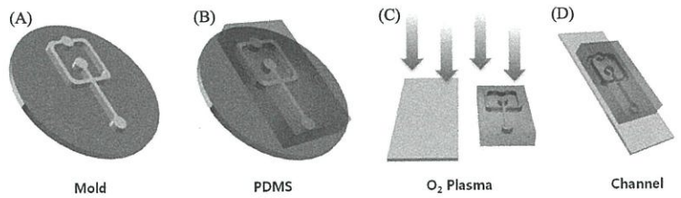

■ **FIGURE 3.3** Preparation process of a PDMS microfluidic channel for the synthesis of PEG microbeads [4].

For the manufacturing of PEG microbeads using the PDMS cross-junction microfluidic channel, the mixture of hexadecane and sorbitanmonooleate (10:1 ratio) was used as a continuous phase (CP) solution in the channel [9,10]. A dispersed phase (DP) solution was a mixture of PEG-DA and 2-hydroxy-1-[4-(hydroxyethoxy) phenyl]-2-methylpropan (10:1.5 ratio). The flow rates of CP and DP in the channel were controlled by syringe pumps. After the generation of the spherical PEG microdroplets, a curing process was performed using UV irradiation for several milliseconds. Finally, PEG microbeads were obtained through microdroplet synthesis and the UV curing procedure, where two procedures were performed on an inverted microscope with a UV light source.

In a bacteria-actuated microrobot, bacterial patterning on the surface of the microstructure plays an important role in the directivity and velocity of the microrobot. The bacterial patterning method using reactive ion etching (RIE) plasma was proposed [11], where the microrobot with bacterial patterning showed higher velocities than that without bacterial patterning. However, the bacterial patterning method has the limitations of a restricted bacterial attachment and a weak adhesion between the microstructure and the adhesion proteins of the bacteria, such as collagen, fibronectin, or bacteria-specific antibodies. To enhance the velocity of bacteriobots, bacterial attachment was controlled through a selective surface modification of PEG microbeads with PLL (Fig. 3.4) [12]. First, by submerging a half-surface PEG microbead into 1% agarose gel solution, another half surface was exposed. Second, by positioning the exposed surface into the PDMS solution and detaching the PEG microbeads from the agarose, microbeads were transferred to the surface of the PDMS substrate. Third, by soaking the PEG microbeads embedded in the PDMS substrate in a 0.001% PLL solution, then extracting microbeads from the PDMS substrate using ultrasound, the surface modification of the microbeads using PLL was completed. The selectively PLL-coated PEG microbeads showed a controlled bacterial attachment on the restricted surface region (PLL-coated surface). In Fig. 3.5, a different bacterial attachment through the surface modification method

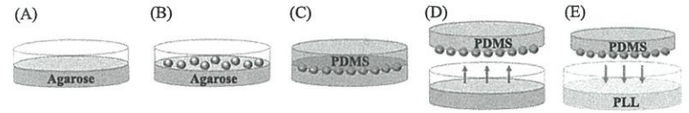

■ **FIGURE 3.4** The modification procedure of PEG microbeads using PLL [12].

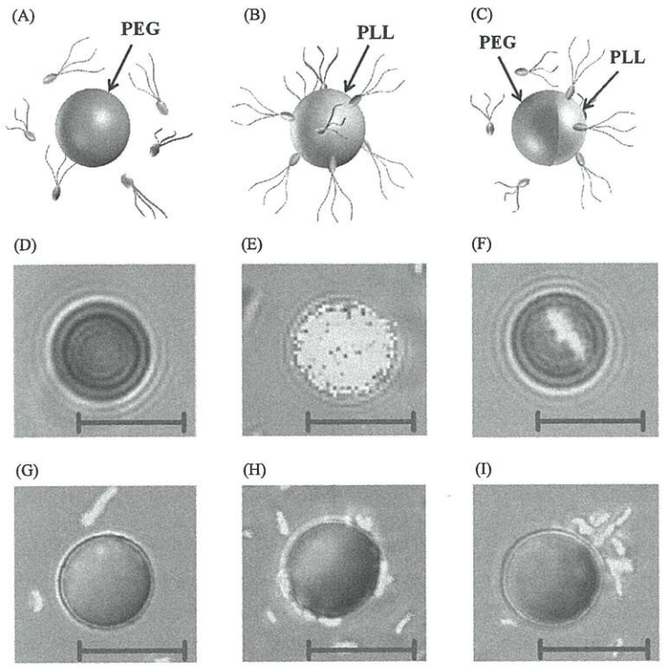

■ **FIGURE 3.5** Confocal laser scanning microscope images of PLL-coated and *S. Typhimurium*-attached PEG microbeads [12].

was described. Non-surface modified PEG microbeads showed no bacterial adhesion, and completely PLL-coated PEG microbeads showed the bacterial adhesion on the entire surface, whereas the selective PLL surface-coated microbeads showed the selective bacterial adhesion on the PLL-coated surface only.

The bacteria-based microrobot, which has a controlled bacterial attachment through selective PLL coating on PEG microbeads, showed an enhanced motility (Fig. 3.6). The bacteria-based microrobot with un-coated PEG microbeads moved at a velocity of 0.03 μm/s and the bacteria-based micro-

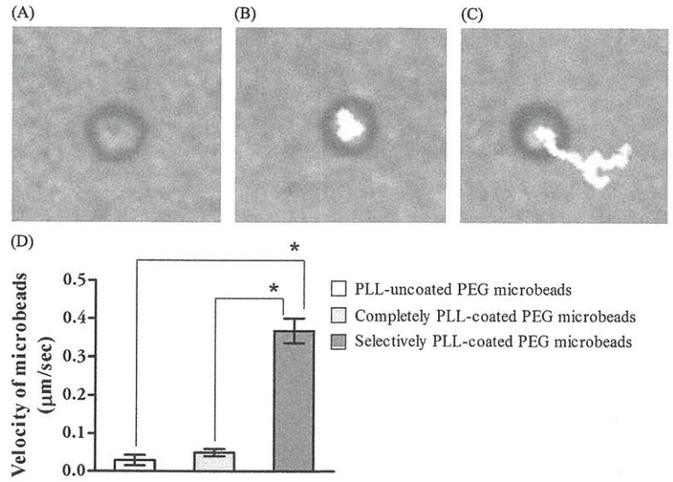

■ **FIGURE 3.6** Comparison of the velocities of bacteria-based microrobots [12].

robot with completely PLL-coated PEG microbeads moved at 0.05 μm/s. However, the bacteria-based microrobot with selectively PLL-coated PEG microbeads moved at a higher velocity of 0.37 μm/s.

3.1.2 Alginate microbeads and surface modification

Alginate is a naturally occurring biopolymer that can be extracted from brown seaweed and has been applied in food and beverage industries as a thickening or gelling agent and a colloidal stabilizer. It can be also used as a matrix for the entrapment and delivery of a variety of drugs and cells in the biotechnology industry, which is due to several properties, including a relatively inert aqueous environment within the matrix, a mild room temperature encapsulation process free of organic solvents, a high gel porosity that allows for high diffusion rates of macromolecules, the ability to control this porosity with simple coating procedures, and the dissolution and biodegradation of the system under normal physiological conditions [13]. In addition, a more effective drug delivery can be achieved through the combination of alginate and chitosan [14]. The complexation of alginate with chitosan can control the release of encapsulated drug or cells by decreasing their leakage. In addition, complexation possesses positive charges that enhance the adhesion of negative charge-surfaced bacteria with alginate microbeads.

The concept of bacteria-based microrobots involves not only a bacteria-actuated drug-embedded microrobot, but also the delivery of therapeutic bacteria themselves. Some genera of bacteria have been proven to accumulate in solid tumors especially, including *Clostridium*, *Bifidus*, and *Salmonella* [15–25]. The administration of engineered *Salmonella Typhimurium*, attenuated and transformed with plasmids encoding the therapeutic gene, caused the localization of *Salmonella* to the tumor tissue and a significant suppression of tumors [24]. However, most of the inoculated bacteria were cleared from the RES system through immunity, and only a little amount of bacteria could reach the target region. If the large number of bacteria was inoculated for a numerical increment of a bacteria reaching at the target site, symptoms related to bacterial infection such as inflammation, toxicity and sepsis may occur [21]. Therefore, many researchers have also focused on the modulation of encapsulation conditions using biodegradable and biocompatible materials with the development of attenuated and genetically modified bacteria strains [26,27]. In this research group, two types of bacteria-based microrobots were developed, which consist of alginate microbeads and attenuated *S. Typhimurium*. The alginate microbead is regarded as cargos of bacteria or drugs, and the attenuated *S. Typhimurium* is adopted as a living therapeutic agent or as an actuator [28]. The alginate microbeads were also manufactured by the micro-droplet generation using a cross-junction microfluidic channel, where the channel fabrication procedure was equal to that for the PEG microbeads. For the synthesis of alginate microbeads, a mixture of mineral oil and sorbitan monooleate (10:1 ratio) was used as a CP solution, and a DP solution consisted of a mixture of 1% alginate and a various number of attenuated *S. Typhimurium*. Through the regulation of the flow rates of CP and DP in the microfluidic channel using a syringe pump, spherical alginate micro-droplets were generated. Then, the solidification of the alginate micro-droplets was performed using 2% $CaCl_2$ located in the outlet part of the microfluidic channel. Finally, the surfaces of the alginate microbeads were coated with chitosan. In the case of encapsulated *S. Typhimurium*, their survival or growth was evaluated through the cultivation of bacteria-encapsulated alginate microbeads in bacterial broth media in a 30°C shaking incubator at various times (0, 6, 12, 18, 24, and 72 h).

The bacteria-encapsulated alginate microbeads with a 1% chitosan coating maintained their structural integrity and showed increments of bacterial growth (Fig. 3.7).

Chitosan-coated alginate microbeads also showed the enhanced attachment of flagellated *S. Typhimurium* on their surface, and the motility of the bacteria-based microrobots was increased (Fig. 3.8).

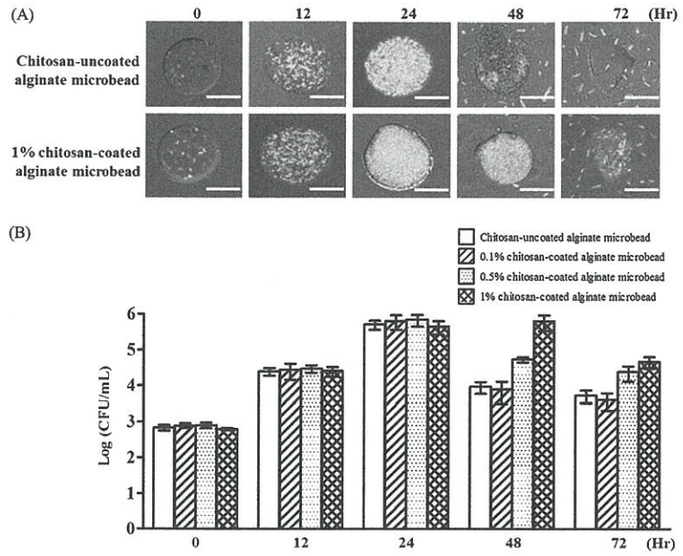

■ **FIGURE 3.7** Improvement of the solidity of bacteria-encapsulated alginate microbeads through surface modification with chitosan [28].

3.2 EVALUATION AND CONTROL OF BACTERIOBOT MOTILITY

In the development of a microrobot, the actuator plays a key role as delivery therapeutic agents or cells into a targeted region. By its nature, the microrobot needs a micro-sized, reliable, and high-efficiency actuator. To solve the limitations of actuators for the microrobot, many research studies have been reported [11,29–31]. For example, Sitti reported a 250 μm × 130 μm × 10 μm-sized neodymium–iron–boron microrobot, which was actuated by six macro-scale electromagnets, able to achieve translation speeds exceeding 10 mm s^{-1} [11]. In addition, Nelson reported artificial bacterial flagella (ABF) consisting of a helical tail like a natural flagellum in size and shape, with a thin square-shaped soft magnetic metal head [31]. The ABF was controlled by three orthogonal electromagnetic coil pairs. However, these systems need complex magnetic coil systems. Meanwhile, flagellated bacteria, such as *Escherichia coli* (*E. coli*), *S. Typhimurium*, and *Serratia marcescens* (*S. marcescens*) were suggested as bioactuators for microrobots [8,32–34]. The flagellated bacteria have many advantages as actuators, including mobile capability using the rotating helical flagella motor with over 100-Hz velocities, the easy acquisition of chemical energy from their environment, and extreme adaptability [8,32–34]. Moreover, some bacteria show taxis phenomena, such as chemotaxis, phototaxis, and magnetotaxis, according to controlling methods, such as chemical gradients, light, and magnetic fields [32].

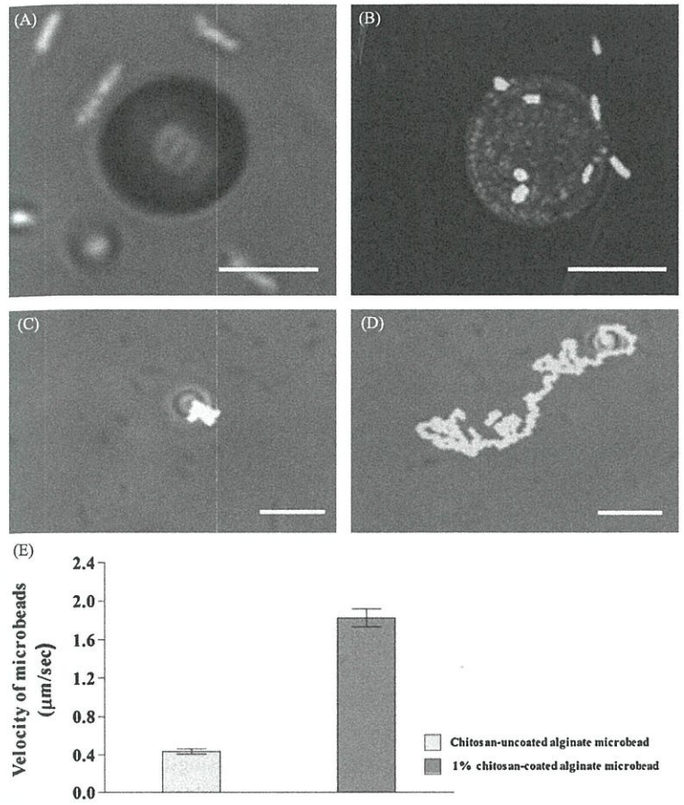

■ **FIGURE 3.8** Comparison of the bacterial attachments on alginate microbeads and the motilities of bacteria-actuated alginate microbeads through surface modification with chitosan [28].

To develop efficient therapeutic bacteriobots using flagellated bacteria as a micro-sized bioactuator, microstructure fabrication, bacterial adhesion, and bacterial patterning were regarded as essential technologies. After the fabrication of the microstructure, the surface of the microstructure was modified by coating with PLL, O_2 plasma, BSA, and biotin. Through the surface modification of microstructures, bacteriobots showed an improved motility through adjusted bacterial adhesion.

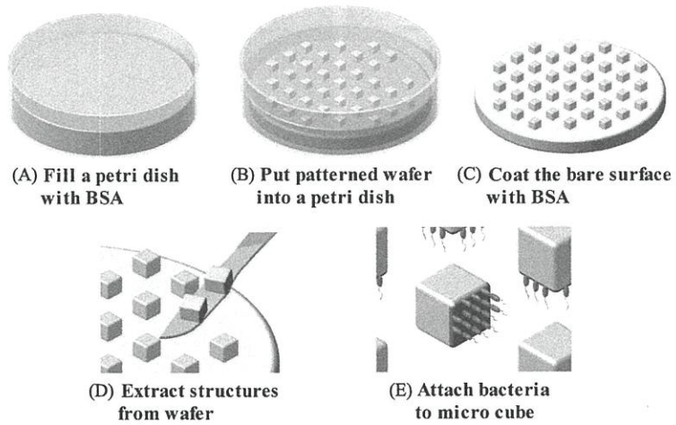

■ **FIGURE 3.9** BSA-selective patterned SU-8 microstructures and bacterial attachment [36].

3.2.1 **Motility control of bacteriobots using BSA**

BSA is known as a non-fouling protein that blocks the adhesion of the bacteria. Using that property, micro-patterning methods of the microstructures were reported. According to Kim et al., the micro patterning of the BSA on the surface of PEG microbeads showed a high bacterial density at 1.48 mg cm^{-2} [35]. Selective BSA-coated microstructures were also fabricated and the bacterial attachment was analyzed [36]. The cube-shaped and micro-sized microstructures were fabricated using the photolithography method with silicon wafer, SU-8, and UV light. For the advanced adhesion of bacteria, SU-8 microstructures and a 5% BSA solution were pre-incubated for 24 h. During incubation, the five faces of the SU-8 microstructure were exposed to BSA. After BSA coating, *S. marcescens* were attached only on the one face of the SU-8 microstructure (Fig. 3.9).

BSA-selective patterned SU-8 microstructures showed different attached bacterial numbers between the BSA coated side and the uncoated side (Fig. 3.10). The bacterial number of the uncoated side in the selectively patterned microstructure was increased by 200% compared with that of the BSA coated side of the microstructure.

According to selective surface patterning, the motility of the bacteria-actuated microstructure was changed. The selectively BSA-coated microstructure showed a 210% higher motility compared to the uncoated microstructure (Fig. 3.11). Consequently, the selective bacterial patterning of

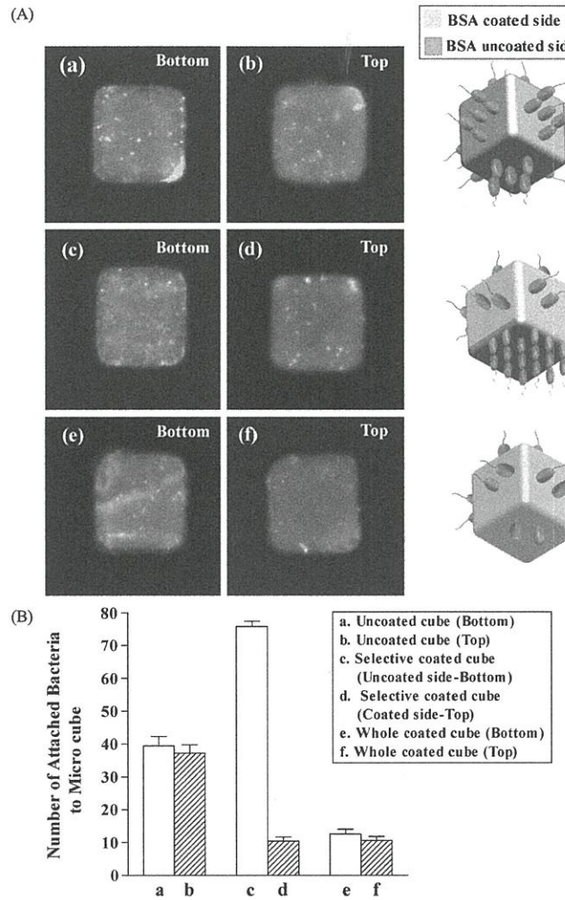

■ **FIGURE 3.10** Comparison of the number of attached bacteria according to BSA selective coating [36].

the microstructure by BSA could significantly enhance the motility of the bacteria-actuated microstructures.

3.2.2 **Motility control of bacteriobot using PLL**

PLL is a positive-charged polymer, which is commonly used for the enhancement of the attachment or immobilization of cells [12], where the positive charge of PLL interacts with the negatively charged cell surface. In this study, bacterial patterning was executed using PLL selective pattern-

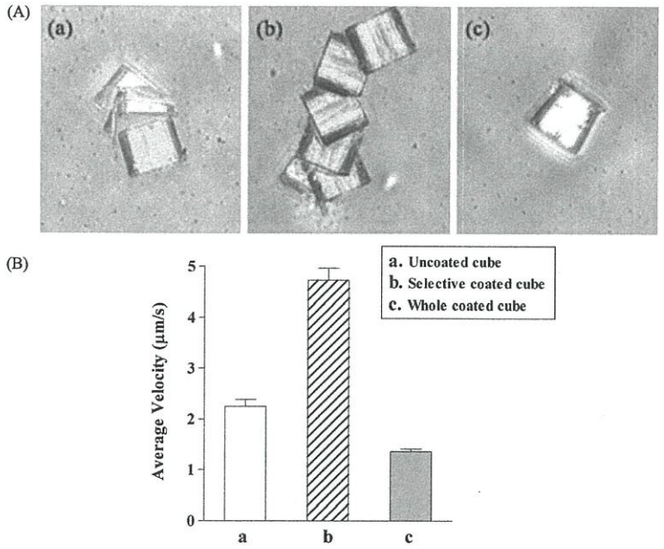

■ **FIGURE 3.11** Images of the movement of cube-shaped microstructures and a comparison of the velocities of microstructures [36].

ing of the microbeads [12]. In addition, the bacterial attachment on the PLL selectively patterned microbeads and the motility of the bacteria-actuated microbeads using PLL selective-patterning microbeads were analyzed (see Section 3.1.1 PEG microbeads and surface modifications).

3.2.3 Motility control of bacteriobot using streptavidin–biotin conjugation

The interaction between streptavidin and biotin is a protein–ligand combination, one of the strongest in nature [37]. Biotin, a small molecular protein, is captured by a tetrameric biotin-binding protein, streptavidin, with a high affinity. This interaction is a widely used tool in biology, such as imaging [38], nano-assembly [39], and pre-targeted cancer immunotherapy [40]. In the development of bacteriobots, for a complete combination of bacteria and the microstructure, biotin molecules were bound to the outer membrane of *S. Typhimurium*, and streptavidin was attached on the surface of the microstructure (Fig. 3.12) [41]. For the fabrication of bacteriobots using the biotin–streptavidin interaction, streptavidin-conjugated tandem fluorochrome was coated on the surface of 3-μm diameter rhodamine-containing fluorescent polystyrene (PS) microbeads by covalent coupling. Through the

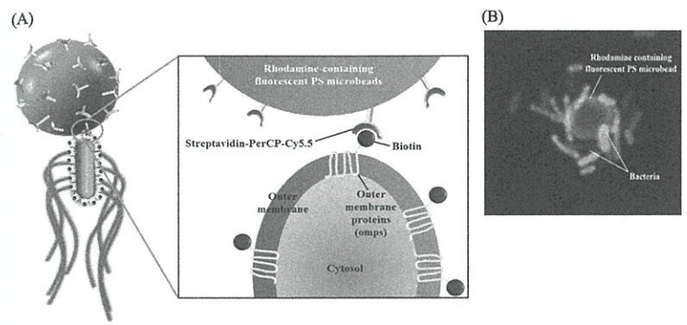

■ **FIGURE 3.12** Development of bacteriobots through the biotin–streptavidin conjugation [41].

incubation of EZ-Link NHS-LC-Biotin with *S. Typhimurium* for 1 h, biotin molecules were combined with the bacterial outer membrane protein (omp). Then, bacteriobots were synthesized through the co-incubation of biotin-labeled *S. Typhimurium* and streptavidin-coated PS microbeads for 30 min. Finally, the fabricated bacteriobot based on the strong biotin–streptavidin conjugation showed a high density of attached bacteria (Fig. 3.12).

3.3 MOTILITY EVALUATION OF THE BACTERIOBOT

The motility of the bacteriobot was regulated by the chemotaxis reaction of the attached bacteria on the microstructure and it was shown as a directional movement toward the chemo-attractant. For the analysis of the motility variation of the bacteriobot, a quantitative evaluation method of the bacteriobot's movement is necessary. The chemotaxis of the *S. marcescens*-based microrobot was reported, and the directional movement of the bacteriobot using *S. marcescens* was analyzed [42,43], which was a simple status verification, not a contained statistical quantification of its directional motility. For the quantitative analysis of the directional movement of the bacteriobot by bacterial chemotaxis, a useful chemotaxis evaluation tool that can create and maintain a concentration gradient of chemotactic inducers was necessary. The evaluation of bacterial chemotaxis using an agar plate method and a capillary method was reported [44]. Through the agar plate method, the direction of bacterial proliferation on a semisolid agar medium was measured simply and conveniently, but not in a liquid medium [45]. Through the capillary method using released chemo-attractants or a chemo-repellent from the capillary tub minutely, the bacterial movement in a liquid medium was measured. This method is also very simple and convenient, but the possible diffusion of chemotactic chemicals in a liquid medium occurred in a

very short time, and it is difficult to measure the chemotaxis of low-motility bacteria [46]. The different evaluation methods using microfluidics, which can generate the concentration gradient of chemo-attractants and identify the motility of bacteria, were proposed by many researchers [47–51]. However, these methods also have some limitations, such as the generation of an irregular concentration gradient, the difficult direct measurement of bacterial motility by flow disturbances, and the difficult evaluation of chemotaxis in low-motility bacteria due to the migration flow, especially. The maintainable span of the chemical gradient is too short to measure the chemotaxis of low-motility bacteria. Consequently, a stable gradient-verification method with a steady gradient sustained and no flow micro channel was needed. Some types of microfluidic chambers were fabricated and the directional movement of the bacteriobot was evaluated.

First, a web-type chamber microfluidic platform was developed, which can continuously sustain a chemical concentration gradient with no flow in a microfluidic chamber (Fig. 3.13) [52]. This web-type microfluidic device was synthesized using conventional photo- and soft- lithography with a web-type microfluidics pattern-embossed SU-8 mold, a PDMS solution, and O_2 plasma for the hardening of PDMS. The fabricated web-type microfluidic chamber showed vertical symmetry, contained arch-shaped and radial-shaped micro-channels of a 200-μm width on the left and right sides that were connected with the center circle of a 2-mm diameter (Fig. 3.13).

The fabricated microfluidic chamber was occupied in the generation of the chemical concentration gradient and used for the evaluation of bacterial or the bacteriobot's distribution using a chemo-repellent ($NiSO_4$) and chemo-attractant (aspartic acid). The bacterial distributions according to the concentration gradient of chemo-effectors were different (Fig. 3.14). Compared with that in the PBS region, the number of *S. Typhimurium* in the aspartic acid gradient region increased by about 16%, but the number of *S. Typhimurium* in the $NiSO_4$ gradient region decreased by about 22%. In addition, the chemotactic motility of the bacteriobot according to the concentration gradient of chemo-effectors was also different. The distribution of bacteriobots was significantly increased in the tumor-attractant region and decreased in the tumor-repellent region (Fig. 3.15). According to these results, the web-type microfluidic chamber was appropriated to evaluate the chemotactic motilities of the bacteria or the bacteriobot.

Another type of chemotactic microfluidic chamber was proposed, which maintains a stable and uniform concentration gradient of chemo-effectors and shows no flow [41]. For the evaluation of the chemotactic motilities of bacteria or bacteriobots, the proposed chamber was suitable for

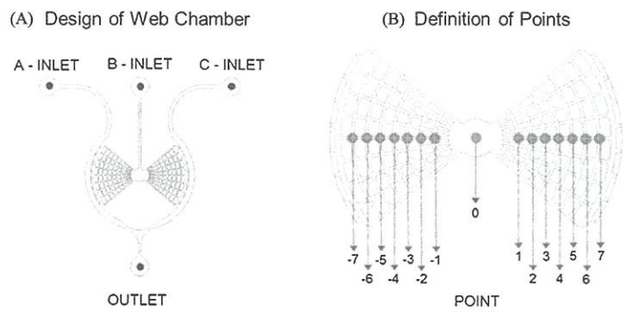

FIGURE 3.13 Development of web-type chamber for the analysis of the movements of bacteria or the bacteriobot [52].

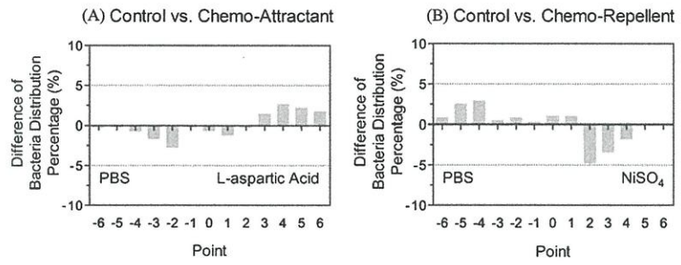

FIGURE 3.14 The different distributions of bacteria according to the concentration gradient of chemo-effectors [52].

the confirmation of the chemotactic movements of bacteria or bacteriobots (Fig. 3.16). This microfluidic device is composed of two chambers for filling tumor cell lysates or spheroids on the left and right sides and a central chamber for loading bacteria or bacteriobots. It provides a concentration gradient through the simple diffusion phenomenon without flow. The microfluidic

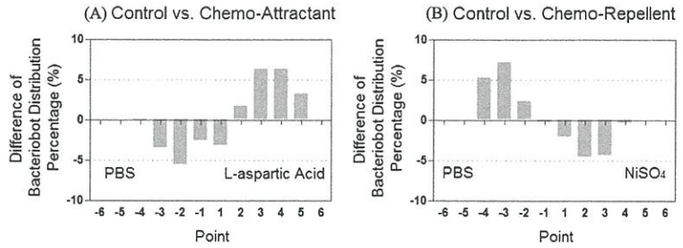

■ **FIGURE 3.15** The different distributions of bacteriobots according to the concentration gradient of chemo-effectors [52].

device was fabricated with a photo-resistor (SU-8) spin-coated wafer, microfluidic channel pattern, PDMS, and O_2 plasma gas. First, the SU-8 mold for the microfluidic device was fabricated by conventional photolithography. Second, the microfluidic device was produced by soft-lithography with an SU-8 mold, PDMS solution, and O_2 plasma.

Using the fabricated microfluidic device, the movements of the bacteria or bacteriobots through chemotactic reactions were evaluated, where the chemical reactions were generated due to the concentration gradients of tumor cell lysates or tumor spheroids (Fig. 3.17). As a result, this type of microfluidic chamber can be a valuable application to estimate the tumor-targeting attributes of bacteria or bacteriobots through measuring the directional moving velocity of bacteria or bacteriobots.

3.4 IN VIVO TEST OF THE TUMOR-TARGETING PROPERTIES OF BACTERIOBOTS

Bacteriobots were fabricated, and therapeutic, flagellated bacteria were incorporated with some types of microstructures in anticipation of the application in the diagnosis and treatment of cancer. Therefore, the final phase and the purpose of the bacteriobot's development is the evaluation of tumor therapeutic properties, such as its tumor-targeting effect and tumor-killing effect. These properties can be verified through in vitro tests using tumor cells, and the tumor-targeting properties of the bacteriobot were already tested in a laboratory through analyzing the movement velocities and assembling of bacteriobots toward the tumor cell lysates or tumor spheroids in the microfluidic chamber environment. However, more specifically, the bacteriobots' therapeutic properties, including tumor-targeting and killing effects, must be re-confirmed on the living body. The bacteria alone or in combination with other therapeutics have been employed in cancer therapy, such as imageable cancer therapy, cytolytic therapy, and radiotherapy [53,

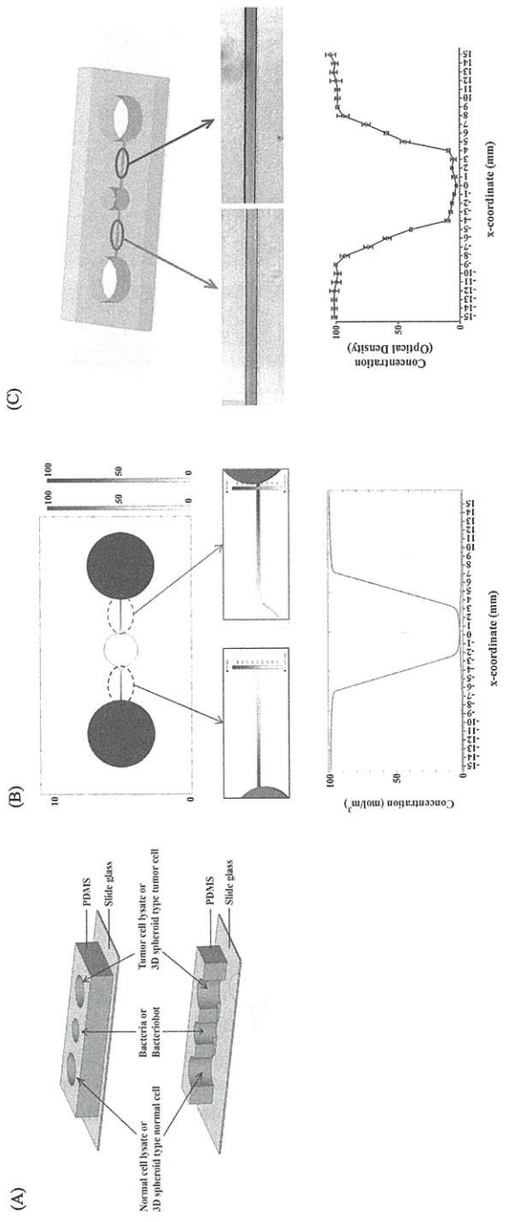

■ **FIGURE 3.16** Schematic diagram of a microfluidic device for the evaluation of the chemotactic movements of bacteria or bacteriobots [41].

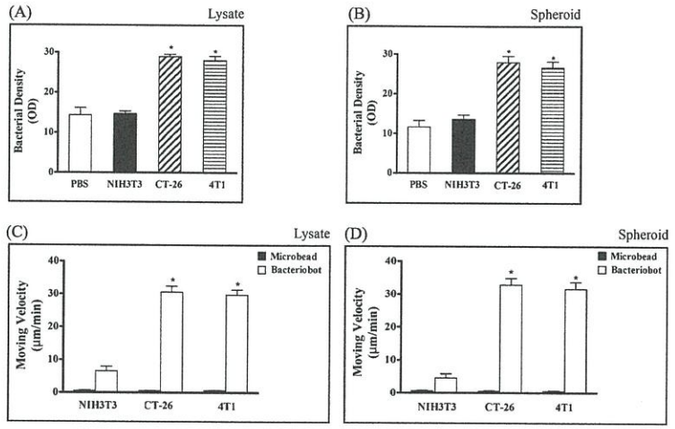

■ **FIGURE 3.17** Demonstration of the tumor-targeting properties of bacteria or bacteriobots using tumor cell lysates and tumor spheroids [41].

54]. These research studies were in vivo investigations of the therapeutic effects of genetically modified bacteria using tumor-bearing mice. However, a bacteriobot was developed using flagellated and chemotactic bacteria as an actuator and microsensor of bacteriobots. An in vivo evaluation of the tumor-targeting properties of the fabricated bacteriobot was executed in a syngeneic mouse tumor model (Fig. 3.18) [41]. First, tumor-bearing mice were prepared through an injection of CT-26 cells (mouse-originated colon cancer cells) subcutaneously. After tumor growth identification, bacteriobots or bacteria and microbeads were injected. Finally, the tumor-targeting properties and localization of bacteriobots were analyzed (Fig. 3.18). From the in vivo test, the bacteriobot was confirmed to target and localize to the CT-26 tumor tissue in the tumor-bearing mice.

3.5 CONCLUSION

This chapter dealt with tumor-targeting bacteriobots, which consist of a microstructure as a micro cargo of the agent imaging or therapeutic agents and flagellated tumor-targeting bacteria as an actuator and sensor. First, the fabrication methods and the surface modification of microstructures were introduced. The microstructures were fabricated using biocompatible materials, such as PLGA, PEG, and alginate. In addition, through coating with PLL, O_2 plasma, BSA, and biotin of the surface structural modifications of microstructures, the bacteriobots showed advanced motility through adjusted bacterial adhesion. Second, a chemotactic motility evaluation method of bacteriobots was developed using the fabricated microfluidic chamber, which can produce a bacterial or bacteriobot distribution gradient by chemotaxis-inducing materials. Finally, the tumor-targeting and localization properties of bacteriobots in tumor-bearing mice were evaluated. Consequently, bacteria-based therapeutic microrobots (bacteriobot) can be considered a new theragnostic methodology for targeted tumor therapy.

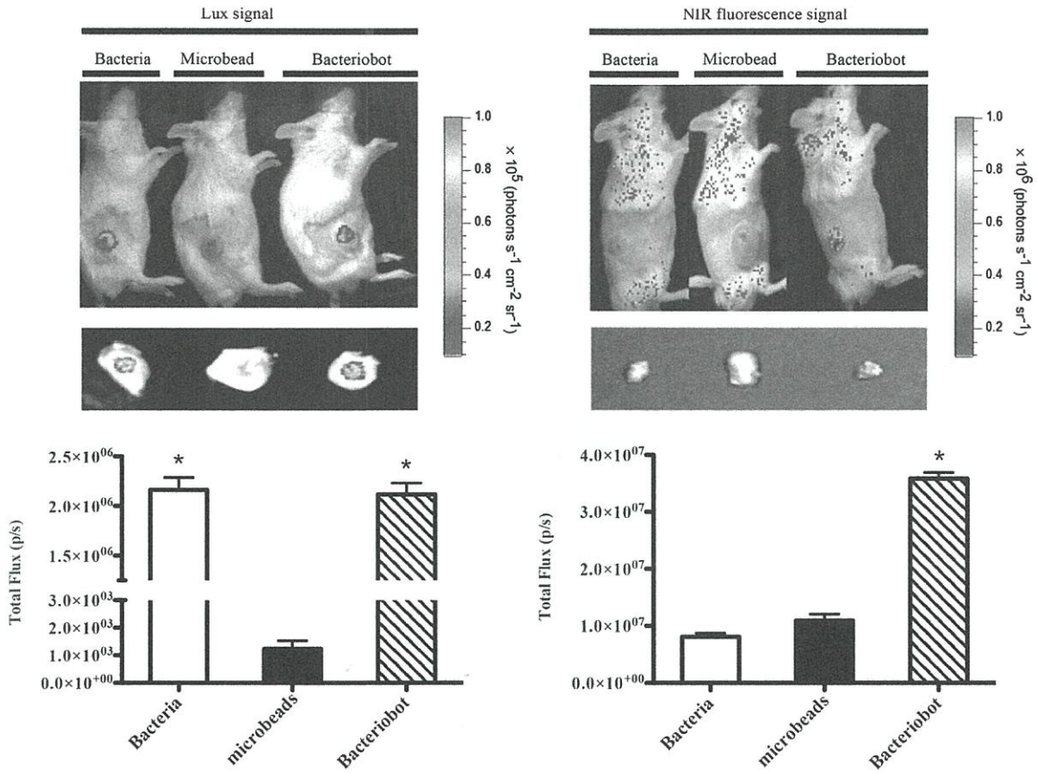

■ **FIGURE 3.18** In vivo tumor-targeting properties of bacteriobots in tumor-bearing mice [41].

REFERENCES

[1] J.W. Chan, C.E. Hoyle, A.B. Lowe, M. Bowman, Nucleophile-initiated thiol-Michael reactions: effect of organocatalyst, thiol, and ene, Macromolecules 43 (2010) 6381–6388.

[2] S. Uthaman, S.H. Cho, I.K. Park, Design and development of biodegradable bacterial-based microrobot for anti-tumour therapy, in: 44th International Symposium on Robotics (ISR), 2013 Oct. 24–26, Seoul (Korea), IEEE Xplore, New York, 2013, pp. 1–4.

[3] C.S. Ki, H. Shih, C.C. Lin, Facile preparation of photodegradable hydrogels by photopolymerization, Polymer 54 (2013) 2115–2122.
[4] J.H. Kim, S.H. Park, D.C. Park, Y.J. Choi, J.O. Park, S.H. Park, Development and evaluation of bacteria based microrobot using biocompatible materials, in: Proceedings of Automobile Research Center Chonnam National University, 2011, pp. 51–54.
[5] M. Rhee, P.M. Valencia, M.I. Rodriguez, R. Langer, O.C. Farokhzad, R. Karnik, Synthesis of size-tunable polymeric nanoparticles enabled by 3D hydrodynamic flow focusing in single-layer microchannels, Adv. Mater. 23 (2011) H79–H83.
[6] G.H.W. Sanders, A. Manz, Chip-based microsystems for genomic and proteomic analysis, Trends Anal. Chem. 19 (2000) 364–378.
[7] T. Ward, M. Faivre, M. Abkarian, H.A. Stone, Microfluidic flow focusing: drop size and scaling in pressure versus flow-rate-driven pumping, Electrophoresis 26 (2005) 3716–3724.
[8] T. Minamino, K. Imada, K. Namba, Molecular motors of the bacterial flagella, Curr. Opin. Struct. Biol. 18 (2008) 693–701.
[9] C.H. Yeh, Y.C. Lin, Using a cross-flow microfluidic chip for monodisperse UV photopolymerized microparticles, Microfluid. Nanofluid. 6 (2009) 277–283.
[10] H. Liu, Y. Zhang, Droplet formation in microfluidic cross-junctions, Phys. Fluids 23 (2011) 082101.
[11] M. Sitti, Miniature devices: voyage of the microrobots, Nature 458 (2009) 1121–1122.
[12] S.H. Cho, S.J. Park, S.Y. Ko, J.O. Park, S.H. Park, Development of bacteria-based microrobot using biocompatible poly (ethylene glycol), Biomed. Microdevices 14 (2012) 1019–1025.
[13] W.R. Gombotz, S.F. Wee, Protein release from alginate matrices, Adv. Drug Deliv. Rev. 31 (1998) 267–285.
[14] R.S. Bhattarai, N.V. Dhandapani, A. Shrestha, Drug delivery using alginate and chitosan beads: an overview, CYC 2 (2011) 192–196.
[15] M. Arakawa, K. Sugiura, H.C. Reilly, C.C. Stock, Oncolytic effect of *Proteus mirabilis* upon tumor-bearing animals. II. Effect on transplantable mouse and rat tumors, Gann 59 (1968) 117–122.
[16] P.K. Bhatnagar, A. Awasthi, J.F. Nomellini, J. Smit, M.R. Suresh, Anti-tumor effects of the bacterium *Caulobacter crescentus* in murine tumor models, Cancer Biol. Ther. 5 (2006) 485–491.
[17] S.H. Kim, F. Castro, Y. Paterson, C. Gravekamp, High efficacy of a Listeria-based vaccine against metastatic breast cancer reveals a dual mode of action, Cancer Res. 69 (2009) 5860–5866.
[18] Y. Kohwi, K. Imai, Z. Tamura, Y. Hashimoto, Antitumor effect of *Bifidobacterium infantis* in mice, Gann 69 (1978) 613–618.
[19] C. Maletzki, M. Linnebacher, B. Kreikemeyer, J. Emmrich, Pancreatic cancer regression by intratumoural injection of live *Streptococcus pyogenes* in a syngeneic mouse model, Gut 57 (2008) 483–491.
[20] R.A. Malmgren, C.C. Flanigan, Localization of the vegetative form of *Clostridium tetani* in mouse tumors following intravenous spore administration, Cancer Res. 15 (1995) 473–478.
[21] N.P. Minton, *Clostridia* in cancer therapy, Nat. Rev. Microbiol. 1 (2003) 237–242.

[22] Z.K. Pan, L.M. Weiskirch, Y. Paterson, Regression of established B16F10 melanoma with a recombinant *Listeria monocytogenes* vaccine, Cancer Res. 59 (1999) 5264–5269.
[23] R.C. Parker, H.C. Plummer, Effect of *histolyticus* infection and toxin on transplantable mouse tumors, Proc. Soc. Exp. Biol. Med. 66 (1947) 461–467.
[24] J.M. Pawelek, K.B. Low, D. Bermudes, Tumor-targeted *Salmonella* as a novel anticancer vector, Cancer Res. 57 (1997) 4537–4544.
[25] Y.A. Yu, S. Shabahang, T.M. Timiryasova, Q. Zhang, R. Beltz, I. Gentschev, W. Goebel, A.A. Szalay, Visualization of tumors and metastases in live animals with bacteria and vaccinia virus encoding light-emitting proteins, Nat. Biotechnol. 22 (2003) 313–320.
[26] J.J. Min, V.H. Nguyen, H.J. Kim, Y.J. Hong, H.E. Choy, Quantitative bioluminescence imaging of tumor-targeting bacteria in living animals, Nat. Protoc. 3 (2008) 629–636.
[27] K. Sultana, G. Godward, N. Reynolds, R. Arumugaswamy, P. Peiris, K. Kailasapathy, Encapsulation of probiotic bacteria with alginate-starch and evaluation of survival in simulated gastrointestinal conditions and in yoghurt, Int. J. Food Microbiol. 62 (2000) 47–55.
[28] S.J. Park, Y.K. Lee, S.H. Cho, S. Uthaman, I.K. Park, J.J. Min, S.Y. Ko, J.O. Park, S.H. Park, Effect of chitosan coating on a bacteria-based alginate microrobot, Biotechnol. Bioeng. 4 (2014) 769–776.
[29] C. Pawashe, S. Floyd, M. Sitti, Modeling and experimental characterization of an untethered magnetic microrobot, Int. J. Robot. Res. 28 (2009) 1077–1094.
[30] H. Choi, J. Choi, G. Jang, J. Park, S. Park, Two-dimensional locomotion of a microrobot with a novel stationary electromagnetic actuation system, Smart Mater. Struct. 18 (2009) 115017.
[31] L. Zhang, J.J. Abbott, L. Dong, B.E. Kratochvil, D. Bell, B.J. Nelson, Artificial bacterial flagella: fabrication and magnetic control, Appl. Phys. Lett. 94 (2009) 064107.
[32] Y. Sowa, R.M. Berry, Bacterial flagellar motor, Rev. Biophys. 41 (2008) 103–132.
[33] M.F. Copeland, D.B. Weibel, Bacterial swarming: a model system for studying dynamic self-assembly, Soft Matter 5 (2009) 1174–1187.
[34] N. Darnton, L. Turner, K. Breuer, H.C. Berg, Moving fluid with bacterial carpets, Biophys. J. 86 (2004) 1863–1870.
[35] D. Kim, W. Lee, W. Koh, Micropatterning of proteins on the surface of three-dimensional poly(ethylene glycol) hydrogel microstructures, Anal. Chim. Acta 609 (2008) 59–65.
[36] S.J. Park, H. Bae, J.H. Kim, B.J. Lim, J.O. Park, S.H. Park, Motility enhancement of bacteria actuated microstructures using selective bacteria adhesion, Lab Chip 10 (2010) 1706–1711.
[37] C.E. Chivers, A.L. Koner, E.D. Lowe, M. Howarth, How the biotin–streptavidin interaction was made even stronger: investigation via crystallography and a chimaeric tetramer, Biochem. J. 435 (2011) 55–63.
[38] M. Howarth, W. Liu, S. Puthenveetil, Y. Zheng, L.F. Marshall, M.M. Schmidt, K.D. Wittrup, M. Bawendi, A.Y. Ting, Monovalent reduced-size quantum dots for single molecule imaging of receptors in living cells, Nat. Methods 5 (2008) 397–399.
[39] M.G. Kattah, J. Coller, R.K. Cheung, N. Oshidary, P.J. Utz, HIT: a versatile proteomics platform for multianalyte phenotyping of cytokines, intracellular proteins and surface molecules, Nat. Med. 14 (2008) 1284–1289.

[40] D.M. Goldenberg, R.M. Sharkey, G. Paganelli, J. Barbet, J.F. Chatal, Antibody pretargeting advances cancer radioimmunodetection and radioimmunotherapy, J. Clin. Oncol. 24 (2006) 823–834.

[41] S.J. Park, S.H. Park, S.H. Cho, D.M. Kim, Y. Lee, S.Y. Ko, Y.J. Hong, H.E. Choy, et al., New paradigm for tumor theranostic methodology using bacteria-based microrobot, Sci. Rep. 3 (2013) 3394.

[42] D. Kim, A. Liu, E. Diller, M. Sitti, Chemotactic steering of bacteria propelled microbeads, Biomed. Microdevices 14 (2012) 1009–1017.

[43] M.A. Traoré, A. Sahari, B. Behkam, Computational and experimental study of chemotaxis of an ensemble of bacteria attached to a microbead, Phys. Rev. E, Stat. Nonlinear Soft Matter Phys. 84 (2011) 061908.

[44] T. Ahmed, R. Stocher, Experimental verification of the behavioral foundation of bacterial transport parameters using microfluidics, Biophys. J. 95 (2008) 4481–4493.

[45] A.J. Wolf, H.C. Berg, Migration of bacteria in semisolid agar, Proc. Natl. Acad. Sci. USA 86 (1989) 6973–6977.

[46] R. Bainer, H. Park, P. Cluzel, A high-throughput capillary assay for bacterial chemotaxis, J. Microbiol. Methods 55 (2003) 315–319.

[47] D.L. Englert, M.D. Manson, A. Jayaraman, Flow-based microfluidic device for quantifying bacterial chemotaxis in stable, competing gradients, Appl. Environ. Microbiol. 75 (2009) 4557–4564.

[48] H. Jeon, Y. Lee, S. Jin, S. Koo, C.S. Lee, J.Y. Yoo, Quantitative analysis of single bacterial chemotaxis using a linear concentration gradient microchannel, Biomed. Microdevices 11 (2009) 1135–1143.

[49] L.M. Lanning, R.M. Ford, T. Long, Bacterial chemotaxis transverse to axial flow in a microfluidic channel, Biotechnol. Bioeng. 100 (2008) 653–663.

[50] H. Mao, P.S. Cremer, M.D. Manson, A sensitive, versatile microfluidic assay for bacterial chemotaxis, Proc. Natl. Acad. Sci. USA 100 (2003) 5449–5454.

[51] R. Stocker, J.R. Seymour, A. Samadani, D.E. Hunt, M.F. Polz, Rapid chemotactic response enables marine bacteria to exploit ephemeral microscale nutrient patches, Proc. Natl. Acad. Sci. USA 105 (2008) 4209–4214.

[52] D.C. Park, S.J. Park, S.H. Cho, Y. Lee, Y.K. Lee, J.J. Min, B.J. Park, S.Y. Ko, J.O. Park, S.H. Park, Motility analysis of bacteria-based microrobot (Bacteriobot) using chemical gradient microchamber, Biotechnol. Bioeng. 111 (2014) 134–143.

[53] V.H. Nguyen, H.S. Kim, J.M. Ha, Y. Hong, H.E. Choy, J.J. Min, Genetically engineered *Salmonella typhimurium* as an imageable therapeutic probe for cancer, Cancer Res. 70 (2010) 18–23.

[54] S.N. Jiang, T.X. Phan, T.K. Nam, V.H. Nguyen, H.S. Kim, H.S. Bom, H.E. Choy, Y.J. Hong, J.J. Min, Inhibition of tumor growth and metastasis by a combination of *Escherichia coli*-mediated cytolytic therapy and radiotherapy, Mol. Ther. 18 (2010) 635–642.